ELSEVIER

Atmospheric Research 75 (2005) 151–166

ATMOSPHERIC RESEARCH

www.elsevier.com/locate/atmos

Analysis of CLIWA-NET intensive operation period data as part of the monitoring activities at the German Meteorological Service site Lindenberg

J. Güldner*, J.-P. Leps

Deutscher Wetterdienst, Meteorologisches Observatorium Lindenberg, OT Lindenberg, Am Observatorium 12, 15848 Tauche, Germany

Received 17 November 2003; received in revised form 13 October 2004; accepted 8 December 2004

Abstract

The improvement of the parameterization of cloud processes with a focus on cloud liquid water and vertical structures of clouds was defined as an important aim of the EU-project CLIWA-NET (Cloud Liquid Water Network). In compliance with its main goals, a ground-based network was established to obtain cloud properties during two intensive operation periods. The Meteorological Observatory Lindenberg was an integrated part of this network performing microwave profiler retrievals and complementary measurements.

In order to provide accurate observations, methods are developed which enable an automatic quality control of microwave radiometer data. The algorithm includes other continuously available measurements from radiosondes and GPS. The access to accurate observations and a routine evaluation of data quality is required for further applications. Assessment of retrieval accuracy and investigations about the diurnal cycle obtained at Lindenberg are presented to exemplify the usefulness of reference sites as an essential component of any observational program. With respect to cloud liquid water estimates, it is shown that the integrated values are in good agreement with calculations derived from radiosondes. The low-resolution liquid water profiles show deviations in cloud base height, especially for fractional cloudiness.

Keywords: Ground-based remote sending; Microwave radiometer; Thermodynamic profiling; Cloud liquid water

* Corresponding author. Fax: +49 33677 60280.
E-mail addresses: juergen.gueldner@dwd.de (J. Güldner), jens-peter.leps@dwd.de (J.-P. Leps).

0169-8095/$ - see front matter © 2005 Elsevier B.V. All rights reserved.
doi:10.1016/j.atmosres.2004.12.007

1. Introduction

The increasing interest in continuous monitoring of the atmospheric boundary layer structure led to the development of a variety of ground-based remote sensing techniques. Accurate independent data sets must be available for numerical forecast models and the validation of satellite derived parameters as well as for climate applications. Especially, the lack of knowledge about clouds results in the fact that improvements in the prediction of clouds and precipitation have made slower progress than prediction of other meteorological parameters.

In view of the limitations of observing cloud liquid water (CLW) and its vertical structure accurately, the EU project CLIWA-NET (Cloud LIquid WAter-NETwork) was initiated to evaluate and improve model cloud parameterization. A detailed description of the specific objectives of CLIWA-NET is given by Crewell et al. (2002, 2003) and the temporary operation of a European Cloud Observation Network (ECON) is stated there as indispensable component of the entire task. In accordance with the project goals and as part of an Earth observing system aimed at obtaining long-term observations, the German Meteorological Service (Deutscher Wetterdienst, DWD) is extending the Meteorological Observatory Lindenberg as a validation site. Such reference stations are essential due to the fact that new algorithms must be checked against independent surface and aircraft in situ or remote sensing observations (Wielicki et al., 1995). In addition to acquiring long-term data sets, the operation of the reference station permits the generation of data products of higher levels, the assessment of the accuracy of observed and calculated data, and the improvement of quality control algorithms.

During two intensive observing periods in August/September 2000 (CNN I, CLIWA-NET Network) and in April/May 2001 (CNN II), 11 stations were operated to provide cloud information. Among other instruments, the participating DWD stations at Lindenberg and Potsdam were equipped with a passive microwave radiometer, ceilometer, and IR radiometer. The measurements and results obtained with the microwave profiler (MWP) TP-WVP 3000 (Solheim et al., 1998) provided the basis for the present study.

2. Application of quality controlled data sets

2.1. Continuous evaluation of retrieval accuracy

Continuous observation of reliable data is the foremost task of any reference station and various inversion techniques have been developed to calculate vertical profiles of atmospheric parameters (Westwater, 1993). Detecting and eliminating faulty observations are not easily accomplished and require targeted algorithms. New methods to minimize errors in microwave radiometer measurements caused by rain have been developed and demonstrated (Ware et al., 2004). Nevertheless, concurrent measurements employing independent techniques are needed for intercomparisons. The reference site at Lindenberg is optimally equipped to assess the data quality of its monitoring products. The Meteorological Observatory Lindenberg (MOL; 52.22°N, 14.12°E) is operated by DWD. It provides aerological in-situ observations and several active and passive

ground-based remote sensing measurements. In order to accomplish the quality control of microwave data and of the corresponding retrieved profiles, an algorithm has been developed which takes into account radiosonde and GPS data. The GPS data were processed at the GeoForschungsZentrum Potsdam (Gendt et al., 2001).

The control scheme realized at the reference site operates partly automatically. Its last step is archiving measurements and results in a databank to complement the "Lindenberg column" (Neisser et al., 2002). With respect to microwave data, measurement errors mostly caused by rain have to be identified and eliminated. Therefore, the IWV (Integrated Water Vapour) calculated from rain-independent radiosonde observations and GPS measurements as well as the variability of consecutive microwave data for the 12 channels are included in the comparison. The evaluation scheme is performed every month after corrected high quality observations of radiosondes are available. The correction method for operational RS80-A humidity profiles used at Lindenberg is described by Leiterer et al. (2005). The algorithm includes groundcheck adjustments, time-lag corrections, and temperature dependent revisions as well as a recognition of icing during the ascent. Compared to research humidity reference radiosondes, the corrected humidity data reveal no significant bias. Firstly, radiosondes are used to correct the bias of IWV derived from GPS measurements for the selected month. For the CLIWA-NET period CNN II, a wet bias of about 0.15 cm was recognized. In contrast to CNN II for CNN I, no significant bias was detected. The IWV retrieved from radiosonde, GPS, and MWP amount to an average of 1.31 cm, 1.46 cm, and 1.30 cm for CNN II and of about 2.15 cm for all methods during CNN I. Thus, the wet bias of GPS data occurs in the drier observation period. The IWV of the MWP is then compared with appropriate radiosonde- and GPS-IWV or the corresponding interpolated values. The influence of the interpolated values on the valuation of quality depends on the time difference to the neighbouring measurements. Together with the variability of MWP measurements, the algorithm allows the automatic elimination of erroneous microwave measurements and resultant retrievals. Data sets perused according to this approach serve as a basis for the following examinations. A schematic diagram of the quality control algorithm is shown in Fig. 1.

The recurrent estimation of retrieval accuracy is a vital component of sounding systems aimed at obtaining long-term observations. In first statistical investigations in 1999 MWP profiles and radiosondes at Lindenberg were compared for 237 cases in summer and 254 cases in winter (Güldner and Spänkuch, 2001). The neural network of Solheim and Godwin (1998) and a statistical regression method which applies interrelated MWP and radiosonde measurements were included in the intercomparisons. The results obtained with the regression method for temperature show that the rms error was about 0.6 K near the surface and less than or equal to 1.6 K up to 7 km height in summer and 4 km height in winter. For water vapour, the corresponding values are 0.2 gm^{-3} near the surface and 0.8–1.0 gm^{-3} from 1 to 2 km height. There was a considerable bias in the water vapour retrievals of the neural network, on average, the retrievals were moister than the radiosonde measurements.

For climate applications, the reliability of results is important. For this reason, the 2-month observation periods of CLIWA-NET have been used to repeat the investigations. The comparison between radiosonde and MWP profiles is shown in Fig. 2 for CNN I and Fig. 3 for CNN II. The curves on the left represent temperature and those on the right show

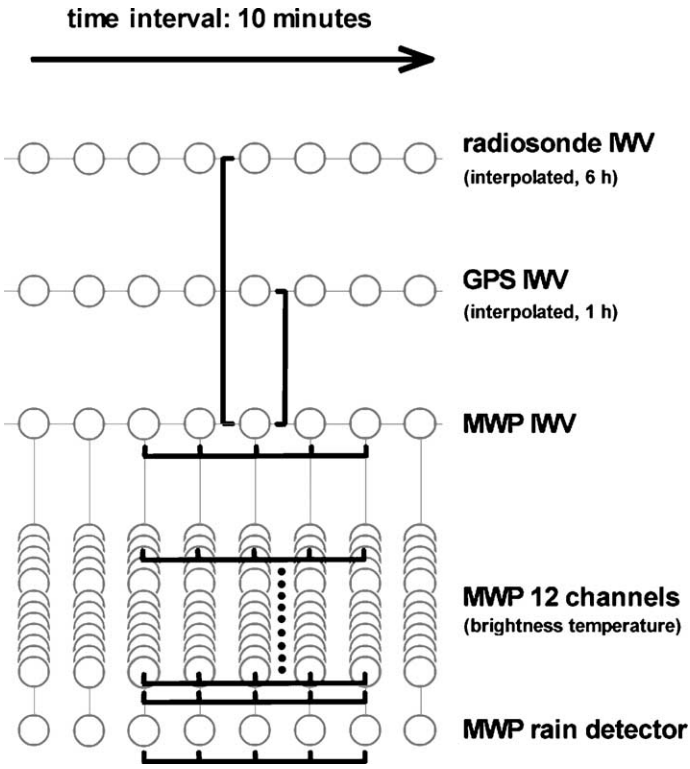

Fig. 1. Diagram of components included in the quality control algorithm. Vertical lines indicate the inclusion of IWV derived from different instruments at a particular time. Horizontal lines denote that temporal variability of measurements is taken into account.

water vapour. The values were calculated from 168 cases during CNN I and 91 cases during CNN II. The standard deviation of the radiosondes is given by thick solid lines; the thin solid lines show the standard deviation of retrieval error for the neural network and the regression method (triangle). The corresponding mean values are reported in Table 1. For the statistical regression, the same operator determined in the earlier study was used. The bias of retrieval results versus radiosonde is given by dotted lines. In essence, the findings affirm the conclusions draw from the first comparison in 1999. The retrieval error that can be expected for temperature is less than 1 K for the lower levels up to 1 km. The standard deviation increases to 1.5–2 K up to 8 km. For water vapour, the corresponding values are less than 0.5 gm^{-3} near the surface and less than 1 gm^{-3} (approximately the half of radiosonde standard deviation) from 1 to 4 km. However, due to the limited vertical resolution caused by smooth weighting function characteristics and the measurement error of the radiosonde as truth reference, their is little scope left to reduce the standard deviation of retrieval error.

Furthermore, it is evident that the neural network overestimates water vapour. It was trained by model calculations, and discrepancies in the radiative transfer model result in the repeatedly detected bias. Statistical regression algorithms avoid this problem because

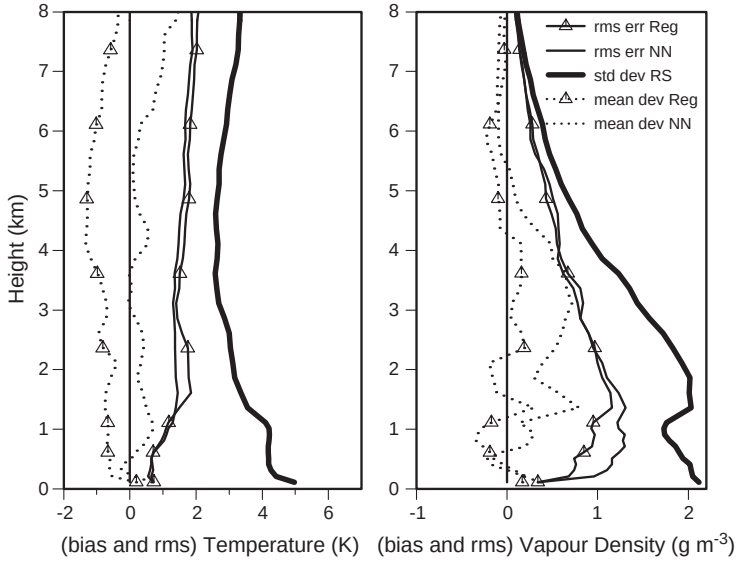

Fig. 2. Retrieval accuracy based on statistical comparison with radiosonde observations during CNN I for 168 cases. The mean differences between radiometer retrievals and radiosondes (MWP-RS) are shown for the regression method (Reg; triangle) and the neural network approach (NN).

radiosonde and simultaneously measured brightness temperatures are used to compute the regression operator. Additionally, long-term observations provide an opportunity to enlarge the basis data set continuously and enable the preparation of different seasonal dependent retrieval methods.

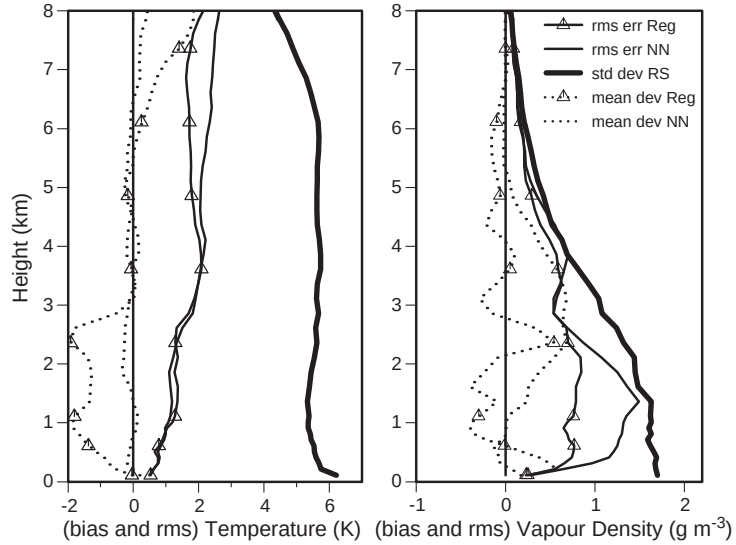

Fig. 3. The same as in Fig. 2 but for 91 cases during CNN II.

Table 1
Mean values of temperature (°C) and vapour density (g m^{-3}) during CNN1 and CNN 2

Height km (NN)	Temperature (°C)		Vapour density (gm^3)	
	CNN 1	CNN 2	CNN 1	CNN 2
0.112	16.2	12.5	10.0	6.8
0.612	14.1	9.7	8.3	5.5
1.112	10.7	5.8	7.1	4.8
1.612	8.0	2.2	5.6	3.9
2.112	5.3	−0.7	4.4	2.9
2.612	3.0	−3.4	3.2	2.2
3.112	0.6	−6.0	2.4	1.6
4.112	−4.9	−12.0	1.4	0.9
5.112	−11.0	−18.6	0.8	0.5
6.112	−17.6	−25.7	0.5	0.3
7.112	−24.8	−33.3	0.3	0.2
8.112	−32.3	−41.1	0.2	0.1

The inherent necessity of a continuous adjustment of retrieval schemes becomes apparent in Figs. 2 and 3 looking at the temperature bias of statistical regression. The retrievals of CNN I and CNN II were carried out with the regression operator developed on the basis of a data set for summer 1999. A 4-month period is seemingly too short to represent the spectra of atmospheric profiles adequately. The temperature standard deviation (regression-radiosonde) was comparable in magnitude to the values retrieved in 1999, whereas a considerable bias is apparent for CNN II in April/May 2001 for the layers up to 2.5 km. The inappropriate regression operator for summer results in underestimated retrieval temperatures during the spring.

The statistical retrieval requires a long record of collocated measurements to avoid the bias evident in the temperature profiles for CNN I and CNN II. Besides the abovementioned inadequate data set, variations in the calibration can cause a bias in the retrieval. The MWP self-calibrates the water vapour channels with continuous tipping curves. For the temperature frequencies of the profiler, an external cold target and the internal ambient target are utilized to calibrate the internal noise diode gain reference. Tipping and cryogenic calibrations are automatically transferred to a temperature stabilized noise source. The V-band noise diode gain reference has been retained unchanged for CNN I and CNN II.

The diversity of error sources proves the necessity of permanent data checks and algorithm adaptions. In this respect, the retrieval acts as an additional calibration algorithm. Appropriate procedures did not exist at the beginning of the CLIWA-NET campaigns, but are performed in current investigations. Quarterly statistics now show a reduced bias.

2.2. Assessment of LWP accuracy

An important objective of CLIWA-NET was to establish a prototype of a cloud observation network. A network implies the ability to operate instruments at a sufficient number of stations. It is obvious that not all stations of the network can provide the

optimum choice of equipment. Particularly, with regard to the limited personnel and material resources, highly sophisticated algorithms as proposed by Han and Westwater (1995), Löhnert and Crewell (2002), and Ware et al. (2003) to retrieve LWC profiles from a combination of microwave and cloud radar measurements can only be applied operationally at a few sites. For this reason, it remains important to provide approximate LWC profiles derived from MWP measurements alone supplemented only by infrared pyrometer and/or laser ceilometer values. The MWP operated at Lindenberg makes use of pyrometer data to obtain information about cloud base temperature. The infrared pyrometer KT19.85, Fa. Heitronics, remotely measures temperature in the 9.6 to 11.5 μm waveband with a 6 degree field of view. The corresponding cloud base altitude is an important constraint in LWC profiling which is accomplished by a neural network. The MWP has a field of view between 5–6° (K-band) and about 2.5° (V-band). Problems with this approach are discussed by Liljegren et al. (2001). The training data set contains LWC profiles and simulated brightness temperatures. A threshold on relative humidity of a radiosonde observation is used to limit liquid water to conforming atmospheric layers. The approach assumes that a cloud fills the field of view of the radiometer (FOVr). The CNN I/II data set is used to investigate limitations of this assumption.

To meet that goal, a special data set was composed containing all available information around the launch time of radiosondes. A classification was performed to separate cloudless cases and to distinguish between fractional and full coverage of clouds in the FOVr. The decision was made manually for each case looking at various cloud-dependent indications. First, the cloud base height detected by the ceilometer was used for the classification. Second, the temperature measured by an infrared pyrometer was taken into account because the measurements reflect the cloud base temperature if the emissivity in the spectral region near 10 μm is close to unity. Additionally, temporal variations of pyrometer values available with a time resolution of one second can be used for the determination of FOVr cloud fraction. A small temporal variability points at a homogeneous cloud base layer and vice versa, partially cloud-filled FOVr causes highly fluctuating pyrometer measurements. A similar approach was used by Coakley and Bretherton (1982) for the determination of cloud fraction from satellite measurements. The spatial coherence method considers the spatial variability of adjacent fields of view to subdivide the clouds. As a third indication to classify the CNN basis data set, the radiosonde observations were used. A threshold of 95% was applied and a cloud was assumed if the relative humidity exceeded this value. Finally, observations by eye of the observer at the meteorological station were integrated. The final result is a cloud fraction classification of available data during the CNN I/II periods around the release time of radiosondes.

A summary figure of cloud base height as a function of the cloud fraction classification is given in Fig. 4 for partial cloudiness and in Fig. 5 for fully cloudy FOVr. The solid boxes denote cloud base height as observed from ceilometer and triangles mark the assigned height of the IR pyrometer value. The number of points is used to indicate the approximate magnitude of liquid water as retrieved from microwave profiler measurements if they are greater than zero. Comparing both figures, a significant difference becomes obvious. For fractional cloud cover examples shown in Fig. 4, the cloud base height of IR pyrometer is noticeable higher than those of ceilometer. The retrieved LWC

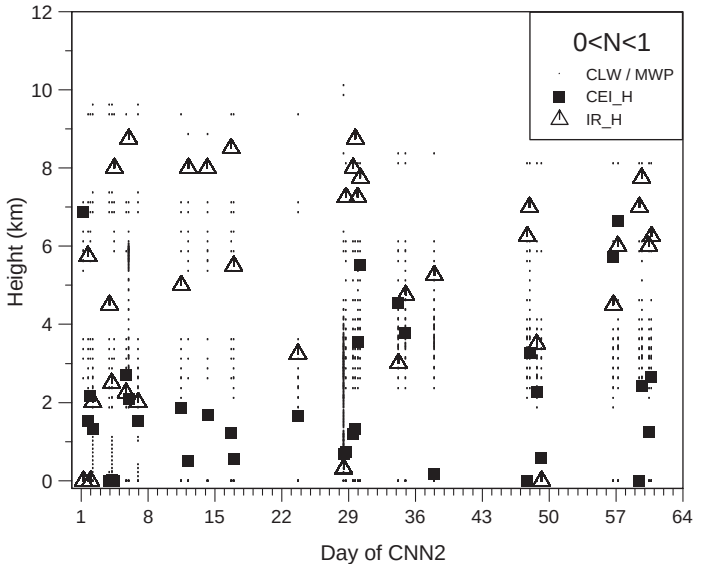

Fig. 4. Cloud base height (CBH) in case of fractional cloud cover. At radiosonde release time, the CBH derived from ceilometer (solid box) and IR pyrometer (triangle) are plotted. The dots indicate non-zero CLW retrieval values.

values appear in-between. On the other hand, all values agree well in general if only comparisons with cloud coverage of N=1 in the FOVr are considered. However, the following problem exists. The retrieved LWC profile is the result of a neural network

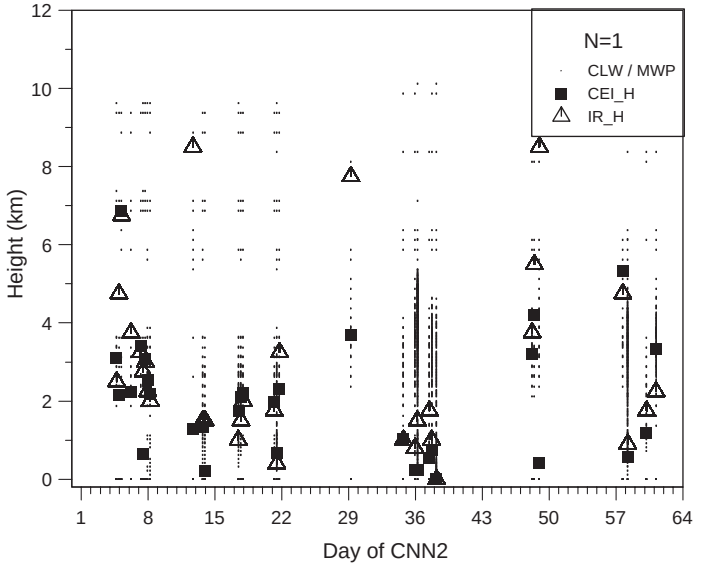

Fig. 5. The same as in Fig. 4 but for total cloud cover.

approach generated on the basis of a training data set. Those data consist of radiosonde observations and corresponding brightness temperature values produced by microwave radiative transfer calculations. Cloud information can be refined by applying a threshold of relative humidity. In either case, full cloudiness is assumed for the creation of a neural network approach. Consequently, the estimation method of liquid water profiles from microwave measurements implies total cloud coverage in the FOVr at a cloud base height as derived from IR pyrometer measurements. If this assumption is not valid, the LWC profiles differ significantly from the ceilometer observations that are assumed to be true. The result of the neural network approach is a trade-off between the overestimated cloud base height and the measured microwave radiation. As can be seen in Fig. 4, the profiling fails often during fractional cloud cover conditions. In contrast, retrievals of total cloud coverage cases produce a much better fit as demonstrated in Fig. 5.

Fig. 6 attempts to clarify the results. It shows scatter plots of cloud base height (CBH) from IR pyrometer and ceilometer versus the height of the lowest significant liquid water content value of the derived MWP profile. The left panel is related to the cases with a partial cloud fraction in the field of view of the radiometer as plotted in Fig. 4. Corresponding to Fig. 5, the right panel shows the CBH for overcast periods. For $N<1$, the difference between the CBH measured by IR pyrometer and ceilometer becomes clearly apparent. The solid line denotes levels of the same CBH. Predominantly, the liquid water content is assigned to heights above the ceilometer measurements and below the values derived from the pyrometer. The MWP retrievals show cloud bases mainly located at 2–3 km height. The results for the data assigned to the group of measurements with total cloud coverage in the FOVr are shown in the right-hand panel. All observations agree well up to 2–3 km height, but the retrieval algorithm does not provide CLW profiles with a cloud

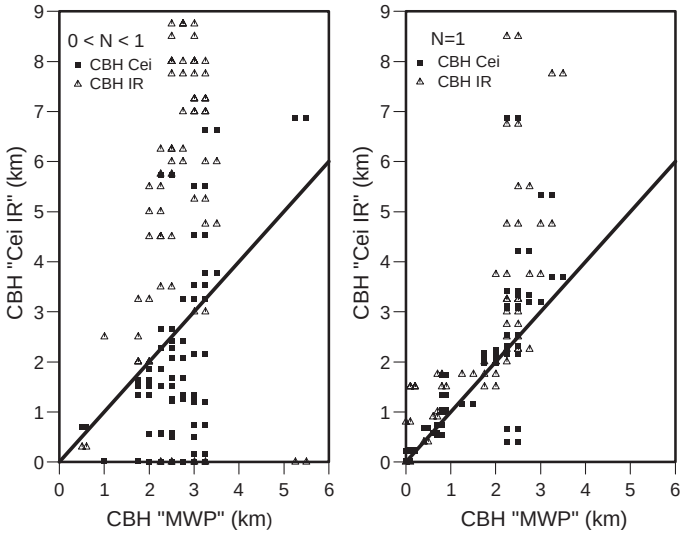

Fig. 6. Cloud base height from ceilometer (solid box) and IR pyrometer (triangle) compared to CBH derived from MWP retrievals of cloud liquid profiles. The observations for (partial/total) cloudiness in the field of view of the radiometer are shown in the (left/right) panel.

base height of more than 3–4 km. Obviously, the information contained in the measured brightness temperature is too weak to generate liquid water at higher levels.

The dependence of retrieval errors on degree of cloudiness is also highlighted in Fig. 7 for CNN I and Fig. 8 for CNN II. CLW profiles were calculated from radiosonde data with a threshold method as described by Löhnert and Crewell (2003). The mean profiles of the estimated CLW are shown in the left panel. The corresponding results of the CLW profiling algorithm are plotted on the right. It is not intended to compare single liquid water profiles but statistical analysis of the prepared data sets can provide information about the potential and the limits of LWC retrieval methods. For both campaign periods, mean CLW profiles of radiosonde display maxima between 1 and 2 km. The MWP retrieved maxima are located considerably higher at about 3 km. For N=1, a secondary maximum appears between the surface and 1 km. This finding is in accordance with Fig. 6. It affirms the potential of the MWP to retrieve liquid water content for lower clouds satisfactorily.

Looking at the integrated values, it is notable that for full cloudiness the integrated values of liquid water are similar. The mean LWP is 0.161/0.175 mm (CNN I/CNNII) for radiosondes and 0.128/0.187 mm (CNN I/CNN II) for MWP retrievals, respectively. This is different than LWP calculated from data sets classified as partially cloud filled in the FOVr. Here, the mean LWP of MWP retrievals (0.069/0.074; CNN I/CNN II) are therefore nearly twice as high as the radiosonde LWP (0.045/0.034; CNN I/CNN II). The reduced LWP during partly cloudy periods is due to the fact that sometimes the radiosonde trajectory is missing the cloud. The resulting ratio can be regarded as rough estimate of the mean degree of cloudiness for the data set representing measurements with partial cloudiness in the FOVr. Although the calculated mean LWP for these data cannot be used to evaluate the liquid water retrieval accuracy, the reduced mean LWP is well recognized by the retrieval algorithm.

The results indicate that, for total cloudy conditions in its field of view, the radiometer can provide useful information, however, for other cloudy cases, subsequent improve-

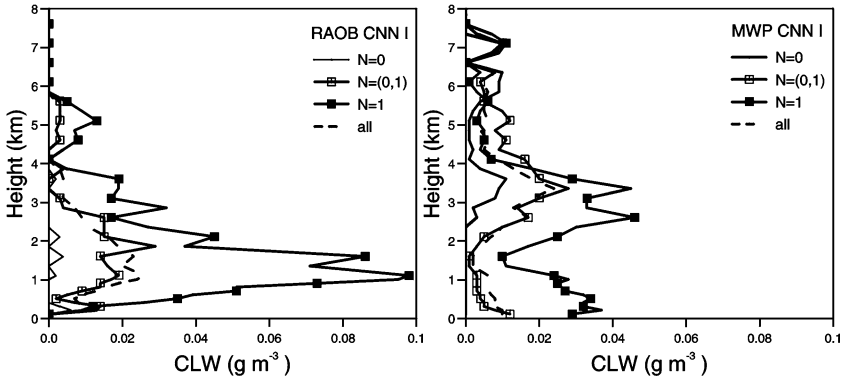

Fig. 7. Mean cloud liquid water (CLW) content for different cloud distributions obtained during CNN I. In the left panel, the CLW calculations based on radiosonde observations are shown. The solid lines display the mean CLW values for the data set for total cloudiness (solid box) or partial cloudiness (box). The mean profile for all cases is given by the dashed line. The right panel shows the corresponding results for the MWP retrievals.

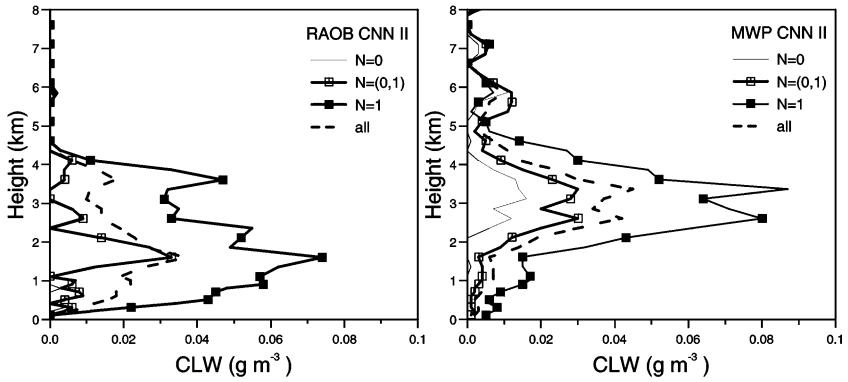

Fig. 8. The same as in Fig. 7 but for CNN II.

ments are required. It is advisable to include ceilometer height in a modified CLW profiling algorithm and to integrate coarse information about the cloud fraction in the FOVr which can be derived from the variability of IR pyrometer measurements. At least a quality flag in dependence of the estimated degree of cloudiness should be provided for other users of CLW retrievals.

2.3. Diurnal variations of temperature and water vapour profiles

Diurnal cycles of temperature and water vapour vertical features are related to many atmospheric processes. They affect the radiation balance and the hydrological cycle. Especially for the highly variable water vapour detailed examinations suffer from coarse temporal resolution of radiosonde observations. With respect to adequate availability of vertical profiles, the situation remains unsatisfactory, even though satellite data have been used increasingly over the past years.

The MWP data sets are available with a temporal resolution of 10 min. Altogether, 7383 (6895) quality controlled temperature and water vapour profiles are archived in the databank during CNN I (CNN II). For this reason, they are well suited for diurnal cycle investigations. It is an additional advantage that measurements were obtained by the same instrument. The profiles were calculated with the same algorithm and proved by means of identical schemes. Similar analysis has been done for the ARM Southern Great Plains site by Wang et al. (2002). GPS-sensed data from 54 sites in North America were used for studying the mean diurnal variations of atmospheric precipitable water (Dai et al., 2002). The observatory at Lindenberg has a long tradition in such investigations. More than 80 years ago, results about the diurnal variation were published (Hergesell, 1922). From May 1917 to June 1919, kite ascents released three times per day were examined. To achieve a uniform distribution of data about the daily hours, the start time was shifted at about 2 h from one day to the next. The replication of diurnal variation analysis for the CNN I and II campaigns reveals the great importance of continuously operating reference stations.

The access to quality controlled data sets greatly facilitates extensive investigations. Using these data, Figs. 9 and 10 were produced where the hourly changes of temperature and vapour density up to 3 km are displayed. The difference of two profiles was taken into

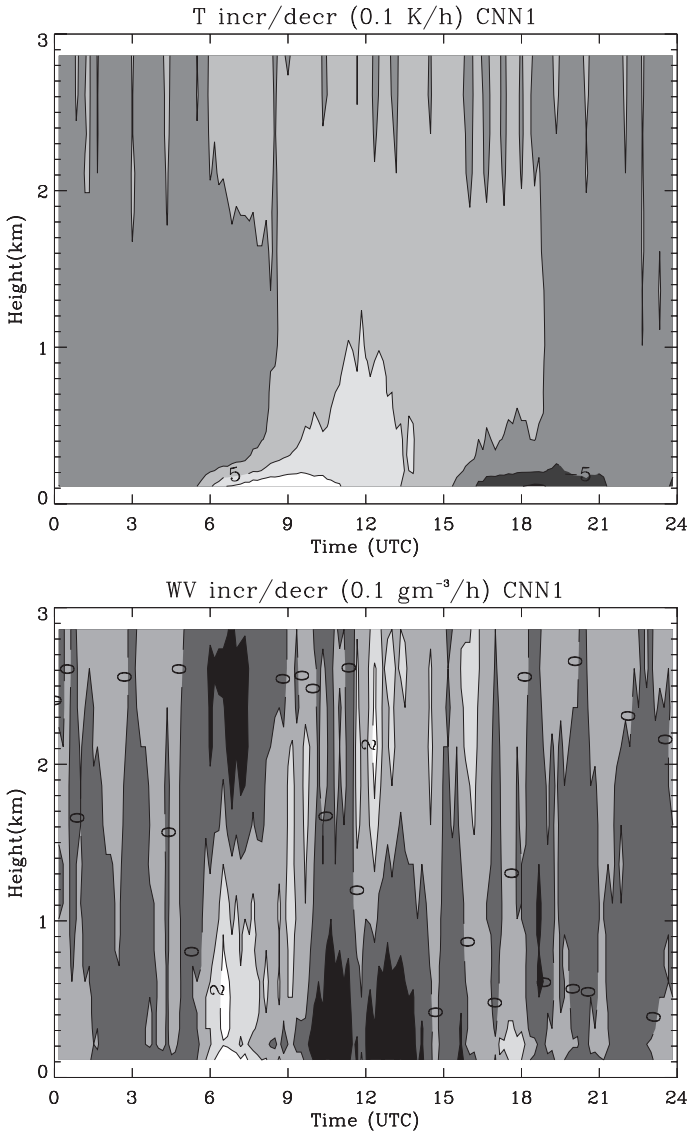

Fig. 9. Diurnal variation of temperature and water vapour during CNN I. Displayed is the mean hourly change of all MWP retrievals passing the quality checks. The bright areas indicate an increase and the dark areas a decrease of temperature and vapour density compared to the corresponding values 1 h before.

account if a profile at a certain point in time and the profile 1 h earlier were both classified as reliable. In the upper panel, the hourly temperature change in tenths of a degree is shown. The light grey and white values in the contour plot indicate an increase of temperature. A decrease is visualized as dark grey and black. The results are displayed versus UTC time. Lindenberg is located at 14.12°E and therefore 0 UTC is equivalent to about 1 o'clock local solar time (LST). In the lower panel, the corresponding hourly

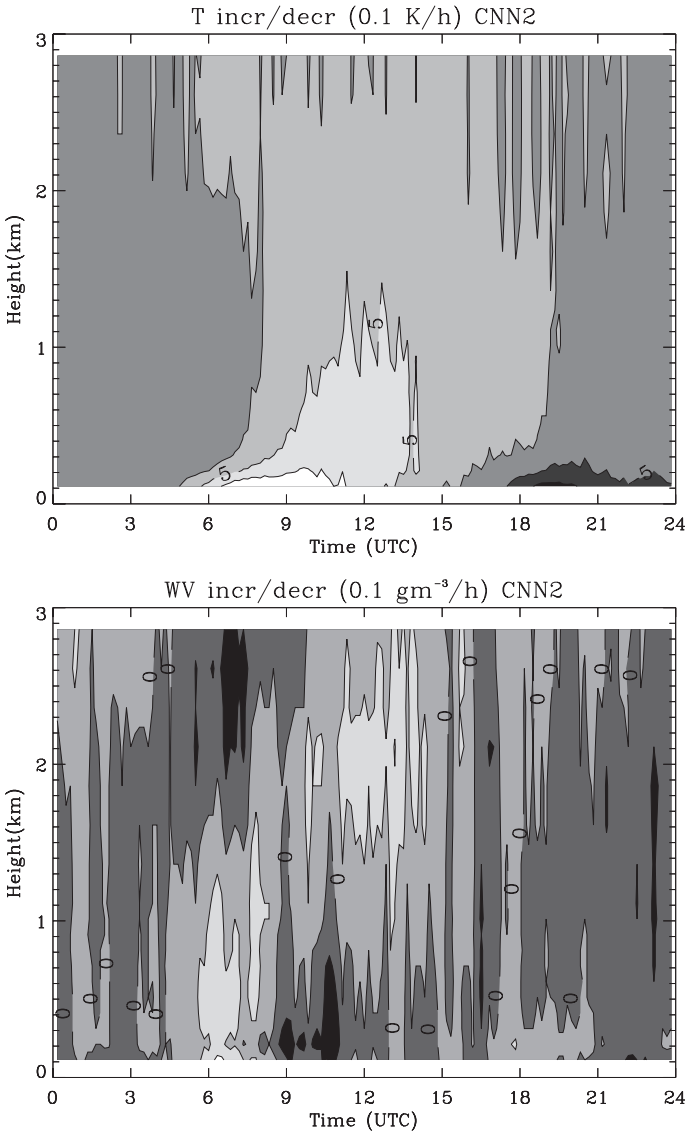

Fig. 10. The same as Fig. 9 but for CNN II.

variability of water vapour in tenths of a gram per cubic meter is plotted. The substantial similarity of the diurnal variation obtained for the different campaign periods is evident and gives reason to assume an underlying physical processes.

The upper parts of Figs. 9 and 10 display explicitly the strong diurnal variation induced by solar heating. They show a minimum near the surface around 6 LST (5 UTC) and a maximum around 16 LST. The temperature minimum occurs 2–3 h later at heights from 0.5 to 2 km. A similar temporal retardation was observed for the maxima. The strongest

mean temperature increase of more than 1 K/h was detected at about 10–11 LST and appears with a delay of up to 3 h at higher vertical levels. The increase decreases with height.

Compared to the temperature changes, the water vapour cycle structure is more variable. It is caused by the multitude of influencing processes such as precipitation, moist convection, and evapotranspiration. Nevertheless, the main anomalies of the different observation periods are in good agreement. As mentioned above, kite ascents had been used to examine diurnal variations in 1917–1919 at the Lindenberg site. Analysis of the water vapour variation led to the conclusion that during summer there are 4 phases (Reger, 1922), including the condensation phase, the evapotranspiration phase, the convection phase, and the advection phase. During the condensation phase until 5 LST, temperature as well as moisture decrease because water vapour condenses as dew. Following the temperature increase thereafter, the mean water vapour density increases simultaneously at heights up to 1.5 km due to evapotranspiration. The increase of water vapour in the lower levels is accompanied by a corresponding decrease in the upper levels.

As described in 1922, moisture reaches a maximum between 9 and 10 LST. The rise in moisture is followed by the convection phase which persists until 15 LST. This phase is characterized by declining values near the surface and a maximum water vapour content at 1.5 to 3 km caused by convection. The beginning of the last phase is marked by repeated increase of moisture mostly as a result of advection. The transition point of time is well pronounced at 15 LST (14 UTC) for CNN I but is poorly defined for CNN II. This example demonstrates the broad applicability of continuous microwave profiler measurements provided that the basis data set is checked and validated by appropriate algorithms.

3. Conclusions

An important objective of the project was to establish a prototype cloud observation network capable of providing data to a broad community of users. The Meteorological Observatory Lindenberg participated in the network created for CLIWA-NET. The existing infrastructure comprising the routine operation of different instruments for vertical sounding was used during the intensive operation periods CNN I and CNN II. The establishment of reference sites is needed as an integral part of any kind of observation program if a continuous validation of measurements and retrievals is required. The advantage of highly developed reference stations was demonstrated for CLIWA-NET. For example, quality control algorithms were developed and applied to reject erroneous measurements of the MWP caused by rain. Accurate values were archived in databanks with a temporal resolution of 10 min. Access to tested data simplifies subsequent investigations. An assessment of retrieval accuracy is possible for any operation period and the calculation of seasonal dependent regression operators is easy to manage. The CNN periods were used to analyse diurnal temperature and water vapour variations. It is intended to extend the data base and repeat the study to include dependence of results on the meteorological background.

The generation of validated data sets for CLW information was another important aim of CLIWA-NET. Observations of the MWP, radiosonde, ceilometer, and IR-pyrometer

were included in the case of this study. It was shown that the accuracy of low-resolution CLW soundings provided by the MWP depends on the cloud fraction in the FOVr. Especially for fractional cloudiness, the assignment of cloud bottom height is unreliable if only one IR-pyrometer measurement is used for the retrieval. A modified algorithm is required taking into account the more precise ceilometer observations. If they are not available, the variability of IR-pyrometer measurements can be used to estimate the cloud fraction and to correct the cloud bottom height. The results obtained at Lindenberg during CNN I and II indicate that a ground-based cloud observation network is feasible. Microwave radiometers are capable of providing information about temperature, water vapour, and cloud liquid water continuously in an unattended mode. Therefore, they are an indispensable component of any observation site in such a network.

Acknowledgements

The authors would like to thank R. Ware for valuable advice and permanent support regarding the operation of radiometers. We also thank U. Löhnert for providing the cloud model and its preparation for application at Lindenberg. The advice of D. Spänkuch and his knowledge about historic studies is greatly appreciated. We would like to thank J. Reichardt for useful comments on the manuscript and the anonymous reviewers for their constructive criticism. Part of this work was performed within the CLIWA-NET project sponsored by the EU under contract number EVK2CT-1999-00007.

References

Coakley Jr., J.A., Bretherton, F.P., 1982. Cloud cover from high resolution scanner data: detecting and allowing for partially filled fields of view. J. Geophys. Res. 87, 4917–4932.

Crewell, S., Drusch, M., van Meijgaard, E., van Lammeren, A., 2002. Cloud observations and modeling within the European BALTEX cloud liquid water network. Boreal Environ. Res. (ISSN: 1239-6095) 7, 235–245.

Crewell, S., Simmer, C., Feijt, A., van Meijgaard, E., 2003. BALTEX BRIDGE cloud liquid water network. Final Report, International BALTEX Secretariat. Publication No. 26, 1–53, ISSN 1681-6471.

Dai, A., Wang, J., Ware, R.H., Van Hove, T., 2002. Diurnal variation in water vapor over North America and its implications for sampling errors in radiosonde humidity. J. Geophys. Res. 107 (D10).

Gendt, G., Reigber, Ch., Dick, G., 2001. Near real-time water vapor estimation in a German GPS network—first results from the ground program of the HGF GASP Projekt. Phys. Chem. Earth 26, 413–416.

Güldner, J., Spänkuch, D., 2001. Remote sensing of the thermodynamic state of the atmospheric boundary layer by ground-based microwave radiometry. J. Atmos. Ocean. Technol. 18, 925–933.

Han, Y., Westwater, E., 1995. Remote sensing of tropospheric water vapor and cloud liquid water by integrated ground-based sensors. J. Atmos. Ocean. Technol. 12, 1050–1059.

Hergesell, M., 1922. Der tägliche Gang der Temperatur in der freien Atmosphäre über Lindenberg. Die Arbeiten des Preußischen Aeronautischen Observatoriums bei Lindenberg. Bd XIV, Wissenschaftliche Abhandlungen 1922, 1–29.

Leiterer, U., Dier, H., Nagel, D., Naebert, T., Althausen, D., Franke, K., Kats, A., Wagner, F., 2005. A correction method for RS80—a humicap humidity profiles and their validation by lidar backscattering profiles in tropical cirrus clouds. J. Atmos. Ocean. Technol. 22, 18–29.

Liljegren, J.C., Clothiaux, E.E., Mace, G.G., Kato, S., Dong, X., 2001. A new retrieval for liquid water path using a ground-based microwave radiometer and measurements of cloud temperature. J. Geophys. Res. 106 (D13), 14485 (2000JD900817).

Löhnert, U., Crewell, S., 2002. Profiling Cloud Liquid by Combination of Multi-Channel Ground-Based Passive Microwave and Cloud Radar Measurements. Proc. Workshop on COST Action 720: Integrated Ground-based Remote Sensing Stations for Atmospheric Profiling, L'Aquela, Italy, pp. 18–21.

Löhnert, U., Crewell, S., 2003. Accuracy of cloud liquid water path from ground-based microwave radiometry 1. Dependency on cloud model statistics. Radio Sci. 38 (3).

Neisser, J., Adam, W., Beyrich, F., Leiterer, U., Steinhagen, H., 2002. Atmospheric boundary layer monitoring at the Meteorological Observatory Lindenberg as a part of the "Lindenberg Column": facilities and selected results. Meteorol. Z. 11 (4), 241–253.

Reger, J., 1922. Der tägliche Gang der Feuchte über Lindenberg. Die Arbeiten des Preußischen Aeronautischen Observatorium bei Lindenberg. Bd XIV, Wissenschaftliche Abhandlungen 1922, 44–61.

Solheim, F., Godwin, J., 1998. Passive ground-based remote sensing of atmospheric temperature, water vapor, and cloud liquid water profiles by a frequency synthesized microwave radiometer. Meteorol. Z. N.F.7, 370–376.

Solheim, F., Godwin, J.R., Westwater, E.R., Han, Y., Keihm, S.J., Marsh, K., Ware, R., 1998. Radiometric profiling of temperature, water vapor and cloud liquid water using various inversion methods. Radio Sci. 33, 3404–3932.

Wang, J., Dai, A., Carlson, D.J., Ware, R.H., Liljegren, J.C., 2002. Diurnal Variation in Water Vapor and Liquid Water Profiles from a New Microwave Radiometer Profiler. Sixth Symposium on Integrated Observing System, 13–18, January 2002, Orlando, Florida, pp. 198–201.

Ware, R., Carpenter, R., Güldner, J., Liljegren, J., Nehrkorn, T., Solheim, F., Vandenberghe, F., 2003. A multichannel radiometric profiler of temperature, humidity and cloud liquid. Radio Sci. 38 (4), 8079.

Ware, R., Cimini, D., Herzegh, P., Marzano, F., Vivekanandan, J., Westwater, E., 2004. Ground-Based Microwave Radiometer Measurements During Precipitation. 8th Specialist Meeting on Microwave Radiometry, 24–27 Feb 2004, Rome, Italy.

Westwater, E.R., 1993. Ground-based microwave remote sensing of meteorological variables. In: Janssen, M.A. (Ed.), Atmospheric Remote Sensing by Microwave Radiometry. Wiley, New York, pp. 145–213.

Wielicki, B.A., Cess, R.D., King, M.D., Randall, D.A., Harrison, E.F., 1995. Mission to planet earth: role of cloud and radiation in climate. Bull. Am. Meteorol. Soc. 76, 2125–2153.